Published in final edited form as:
Prostate. 2014 June ; 74(8): 869–879. doi:10.1002/pros.22805.

Interleukin-17 promotes development of castration-resistant prostate cancer potentially through creating an immunotolerant and pro-angiogenic tumor microenvironment

Qiuyang Zhang[1], **Sen Liu**[1], **Qingsong Zhang**[1,2], **Zhenggang Xiong**[6], **Alun R. Wang**[6], **Leann Myers**[7], **Jonathan Melamed**[8], **Wendell W. Tang**[9], and **Zongbing You**[1,2,3,4,5,*]

[1]Department of Structural & Cellular Biology, Tulane University, New Orleans, Louisiana 70112

[2]Department of Orthopaedic Surgery, Tulane University, New Orleans, Louisiana 70112

[3]Tulane Cancer Center and Louisiana Cancer Research Consortium, Tulane University, New Orleans, Louisiana 70112

[4]Tulane Center for Stem Cell Research and Regenerative Medicine, Tulane University, New Orleans, Louisiana 70112

[5]Tulane Center for Aging, Tulane University, New Orleans, Louisiana 70112

[6]Department of Pathology and Laboratory Medicine, School of Medicine, Tulane University, New Orleans, Louisiana 70112

[7]Department of Biostatistics and Bioinformatics, School of Public Health and Tropical Medicine, Tulane University, New Orleans, Louisiana 70112

[8]Department of Pathology, New York University School of Medicine, New York, New York 10016

[9]Department of Pathology, Ochsner Clinic Foundation, New Orleans, Louisiana 70121

Abstract

BACKGROUND—Interleukin-17 (IL-17) has been demonstrated to promote formation and growth of hormone-naïve prostate adenocarcinoma in mice. IL-17's role in development of castration-resistant prostate cancer is unknown. In the present study, we investigated IL-17's role in castration-resistant prostate cancer in a mouse model.

METHODS—IL-17 receptor C (IL-17RC) deficient mice were interbred with *Pten* conditional mutant mice to produce RC^+ mice that maintained IL-17RC expression and RC^- mice that were IL-17RC deficient. Male RC^+ and RC^- mice were *Pten*-null and were castrated at 16 weeks of age when invasive prostate cancer had already formed. At 30 weeks of age, all male mice were analyzed for the prostate phenotypes.

RESULTS—RC^- mice displayed prostates that were smaller than RC^+ mice. Approximately 23% of prostatic glands in RC^- mice, in contrast to 65% of prostatic glands in RC^+ mice, developed invasive adenocarcinomas. Compared to castrate RC^+ mice, castrate RC^- mouse prostate had

[*]Corresponding Author: Zongbing You, Department of Structural & Cellular Biology, Tulane University School of Medicine, 1430 Tulane Ave SL 49, New Orleans, LA 70112; Phone: 504-988-0467; FAX: 504-988-1687; zyou@tulane.edu.

lower rates of cellular proliferation and higher rates of apoptosis as well as lower levels of MMP7, YBX1, MTA1, and UBE2C proteins. In addition, castrate RC^{-} mouse prostate had less angiogenesis, which was associated with decreased levels of COX-2 and VEGF. Moreover, castrate RC^{-} mouse prostate had fewer inflammatory cells including lymphocytes, myeloid-derived suppressor cells, and macrophages.

CONCLUSIONS—Taken together, our findings suggest that IL-17 promotes development of invasive prostate adenocarcinomas under castrate conditions, potentially through creating an immunotolerant and pro-angiogenic tumor microenvironment.

Keywords

Prostate cancer; castration-resistant; interleukin-17; tumor immunology; tumor microenvironment

INTRODUCTION

Locally confined prostate cancer is treated by surgery or radiation. At the advanced stage when metastases occur, prostate cancer is treated with androgen deprivation therapy. However, Castration-induced regression of tumor is typically followed by re-growth with castrate levels of androgens, a status known as castration-resistant prostate cancer (CRPC) [1]. The mechanisms of how hormone-sensitive prostate cancer develops into CRPC remain to be defined. Alterations of androgen receptor (AR) signaling pathways, such as *AR* gene amplification, increase in AR expression, and *AR* gene mutations [2], may cause hypersensitivity of AR to low levels of both endocrine and intracrine androgens [3]. AR splicing variants may constitutively activate AR signaling in ligand-independent manners [4]. AR signaling may also be activated by growth factors in the absence of androgens [5]. Activation of HER-2/neu and Ras/mitogen-activated protein kinase pathways causes androgen-independent AR activities [6]. Transcriptional coactivators may lead to ligand-independent AR activation [7]. Focal neuroendocrine differentiation seems to be a common feature of prostate cancer. By secretion of a number of growth factor-like molecules (such as bombesin, calcitonin, and parathyroid hormone-related peptide), neuroendocrine cells can support the growth and progression of surrounding prostate cancer cells towards the castration-resistant state [8]. Androgen ablation up-regulates expression of the anti-apoptotic *Bcl-2* gene [9] and *clusterin* gene [10], whereas the pro-apoptotic *p53* gene is often mutated [11]. Decreased PTEN or increased Akt activities are linked to castration-resistant progression of prostate cancer [12,13]. Expression of TMPRSS2-ERG (transmembrane protease, serine 2 - E-twenty six related gene) fusion protein [14,15] and some microRNAs [16,17] has also been associated with CRPC.

Interleukin-6 (IL-6) and IL-8 have been found to play a role in development of CRPC [18,19]. Both IL-6 and IL-8 are downstream targets of IL-17, a cytokine that is produced by T_H17 cells, γδ T cells, and other immune cells [20]. IL-17 acts through a heterodimer of receptors IL-17RA and IL-17RC [21–23], thus, either *Il17ra* knockout (KO) or *Il17rc* KO completely abolishes IL-17 signaling [24,25]. We have previously reported that IL-17RC protein expression as detected by the anti-IL-17RC intracellular domain antibodies is significantly increased in CRPC, compared to hormone-sensitive prostate cancer [26,27]. Recently, we cross-bred *Il17rc* KO (*Il17rc*$^{-/-}$) mice with *Pten* conditional KO mice

($Pten^{L/L}$;Cre^{+}) and found that, in *Pten*-deficient context, *Il17rc* KO mice developed significantly smaller prostate tumors compared to *Il17rc* wild-type mice [28]. Our findings suggest that IL-17 promotes formation and growth of hormone-naïve prostate adenocarcinoma. However, it is unknown whether IL-17 plays any role in the development of CRPC. In the present study, we castrated the mice at 16 weeks of age and examined them at 30 weeks of age. We found that *Il17rc* KO mice developed significantly smaller prostates compared to *Il17rc* wild-type mice under castrate conditions.

MATERIALS AND METHODS

Mice

Animal protocol was approved by the Animal Care and Use Committee of Tulane University. The breeding strategy and genotyping protocols have been described previously, using $Pten^{loxp/loxp}$ ($Pten^{L/L}$) mice, PB-Cre4 mice, and $Il17rc^{-/-}$ mice [28]. Male RC^{+} (n = 9) and RC^{-} (n = 9) mice at 16 weeks of age were castrated. This age was chosen because a majority of RC^{+} and RC^{-} mice had already developed invasive adenocarcinomas by this age [28,29]. The castration procedures were as the following: mice were anesthetized with 4% isoflurane; the skin over the scrotum was disinfected by 70% ethanol and Betadine solution; a 0.5-cm incision was made over the scrotum; the testes were exposed by pulling the adipose tissue; a hemostat was applied to curtail blood flow followed by silk ligation of blood vessels; the ductus deferentes were ligated and cut; the testes were excised; and the skin incision was closed with #5-0 nylon suture that was removed 7 days later. All instruments used were sterile. To alleviate pain, Carprofen (2 mg/kg) was injected subcutaneously at the end of surgical procedure and then every 12 hours up to 48 hours.

Histopathology

Mice were euthanized and weighed at 30 weeks of age. The genitourinary (GU) blocs were photographed, weighed with an empty bladder, and fixed *en bloc* as described previously [28,30]. Twenty-eight consecutive 4-μm sections of each prostate were cut and 4 sections (from every seventh section) were stained with hematoxylin and eosin (H&E) for histopathologic assessment in a blinded fashion according to the Bar Harbor Classification [30]. The prostatic glands were assessed under low- and high-power magnifications, and approximately 27 to 94 prostatic glands in each prostate were counted, with a total of over 500 prostatic glands in 9 mouse prostates per genotype. The number of inflammatory cells in the connective tissue space between the prostatic glands was counted in ten high-power fields (x400 magnification) of each dorsal prostatic lobe; the average number of inflammatory cells per high-power field in 9 mouse prostates per genotype was compared.

Immunohistochemical and terminal deoxynucleotidyl transferase-mediated dUTP nick end labeling staining

Immunohistochemical staining and double immunofluorescent staining were performed as described previously [28]. The antibodies used were: rabbit anti-p-Akt (1:100), mouse anti-PTEN (26H9, 1:50), rabbit anti-YB1 (D299, 1:50), and rabbit anti-MTA1 (D40D1, 1:25) from Cell Signaling Technology, Inc., Danvers, MA, USA; rabbit anti-Ki-67 (1:100, EMD Millipore, Billerica, MA, USA); rabbit anti-VEGF (A-20, sc-152, 1:200), goat anti-HIF-1α

(Y-15, sc-12542, 1: 50), rabbit anti-NOS2 (iNOS, N-20, sc-651, 1:100), rabbit anti-Integrin αM (CD11b, H-61, sc-28664, 1:100), goat anti-Ly6C (P-12, sc-23080, 1:100), goat anti-Ly6G (Y-11, sc-103603, 1:100), goat anti-arginase I (V-20, sc-18345, 1:100), and goat anti-COX-2 (C-20, sc-1745, 1:200) from Santa Cruz Biotechnology, Inc., Santa Cruz, CA, USA; rabbit anti-CD31 (Ab28364, 1:50, Abcam, PLC., Cambridge, MA, USA); rabbit anti-laminin (1:100, Sigma-Aldrich, St. Louis, MO, USA); rabbit anti-α-smooth muscle actin (1:200, Pierce Biotechnology, Rockford, IL, USA); goat anti-MMP7 (1:200, R&D systems, Minneapolis, MN, USA); rabbit anti-UbcH10/UBE2C (1:200, Boston Biochem, Cambridge, MA, USA); and Cy3-conjugated anti-goat IgG and DyLight 488-conjugated anti-rabbit IgG (Jackson ImmunoResearch Laboratories, Inc., West Grove, PA, USA). Terminal deoxynucleotidyl transferase-mediated dUTP nick end labeling (TUNEL) staining was performed using TACS.XL® Blue Label *In Situ* Apoptosis Detection Kits (Trevigen, Inc., Gaithersburg, MD, USA) according to the manufacturer's instructions [28]. To quantify Ki-67-positive and TUNEL-positive cells, three animals from each genotype group were randomly selected; three representative prostate sections from each animal were stained; approximately 200 cells per field of ten high-power fields (x400 magnification) of each prostate lobe were counted; and the percentages of positive cells were calculated as the number of positive cells divided by the total number of cells. The density of microvessels was evaluated by counting the CD31-positive microvessels in ten high-power fields per lobe; the average number of CD31-positive microvessels per high-power field in three random mouse prostates per genotype was compared. The myeloid-derived suppressor cells (MDSCs) were defined as CD11b/Gr-1 (CD11b/Ly6C and CD11b/Ly6G) double positive cells. The M1 and M2 macrophages were defined as iNOS-positive and arginase I-positive cells, respectively. The numbers of MDSCs, M1 macrophages, and M2 macrophages in the connective tissue space between the prostatic glands were counted in ten high-power fields (x400 magnification) in each dorsal prostatic lobe; the average numbers of MDSCs, M1 and M2 macrophages per high-power field in three random mouse prostates per genotype were compared.

Statistical analysis

Comparisons of the GU-bloc weights were analyzed using Student's *t* test. Kruskal -Wallis test was used to compare the incidences of normal, PIN and invasive adenocarcinoma. Student's *t* test was used to analyze the remaining data.

RESULTS

Castrate RC^{-} mice developed smaller prostate glands than castrate RC^{+} mice

Previously we found that there were no significant differences in the expression of *Il17rc* mRNA and protein, GU-bloc weight, and histopathology between *Il17rc*$^{+/+}$;*Pten*$^{L/L}$;Cre^{+} and *Il17rc*$^{+/-}$;*Pten*$^{L/L}$;Cre^{+} mice [28]. Therefore, we put *Il17rc*$^{+/+}$;*Pten*$^{L/L}$;Cre^{+} mice and *Il17rc*$^{+/-}$;*Pten*$^{L/L}$;Cre^{+} mice into one group, named RC^{+} mice that expressed IL-17RC receptor. Likewise, *Il17rc*$^{-/-}$;*Pten*$^{L/L}$;Cre^{+} mice were named RC^{-} mice that did not express IL-17RC receptor. Both RC^{+} and RC^{-} mice had *Pten* gene conditionally knocked out in the prostatic epithelium due to probasin promoter-driven Cre recombinase [28]. We reported that the GU blocs, including the prostatic glands, were clearly larger in the non-castrate (or

intact) RC^+ mice than in the intact RC^- mice at 30 weeks of age (Fig. 1A and 1B) [28]. In the present study, we found that the GU blocs also appeared larger in the castrate RC^+ mice than in the castrate RC^- mice at 30 weeks of age (Fig. 1C and 1D). The average GU bloc weight was 946.3 mg in the intact RC^+ mice compared to 644.7 mg in the intact RC^- mice ($P < 0.01$, Fig. 1E). Castration at 16 weeks of age significantly reduced the GU bloc weight at 30 weeks of age in both RC^+ and RC^- mice to an average of 224.1 mg and 164.3 mg, respectively ($P < 0.01$, Fig. 1E). Yet, the GU bloc weight of castrate RC^+ mice was still significantly heavier than that of castrate RC^- mice ($P < 0.05$, Fig. 1E).

Castrate RC^- mice developed fewer invasive adenocarcinomas than castrate RC^+ mice

It has been reported that intact RC^+ mice developed invasive adenocarcinomas, that is, the neoplastic cells have invaded through the basement membrane and into the stroma, at 30 weeks of age with 100% penetrance [28,29], whereas intact RC^- mice developed invasive adenocarcinomas in about 70% of prostates at 30 weeks of age [28]. In the castrate RC^+ mice, we found that approximately 65% of prostatic glands presented with invasive adenocarcinomas (Fig. 2A), 33% of prostatic glands had prostatic intraepithelial neoplasia (PIN), and 2% of prostatic glands appeared “normal” as they presented with a single layer of luminal epithelial cells. In contrast, the castrate RC^- mice showed approximately 23% of prostatic glands with invasive adenocarcinomas, 64% of prostatic glands with PIN, and 12% of prostatic glands with normal epithelia (Fig. 2B). Under higher magnification, the invasive adenocarcinoma cells presented with atypical hyperchromatic nuclei and invaded into the surrounding stroma (Fig. 2C and 2D). The rate of invasive adenocarcinomas was 42% lower in RC^- mice than in RC^+ mice ($P < 0.001$, Fig. 2E).

To verify our diagnosis of invasive adenocarcinoma versus PIN based on H&E-stained tissue sections, consecutive sections were stained with H&E and immunohistochemically stained with anti-laminin or anti-α-smooth muscle actin (α-SMA) antibodies. As shown in Supplementary Figure 1A, invasive adenocarinoma showed lack of staining or discontinuity of staining for laminin. In contrast, PIN lesion presented a continuous layer of laminin staining around the prostatic gland (Supplementary Fig. 1B). Similarly, α-SMA staining showed lack of continuity in invasive adenocarcinoma (Supplementary Fig. 1C), whereas a continuous layer of α-SMA staining was present in the PIN lesion and normal gland (Supplementary Fig. 1D).

Castrate RC^- prostate had less cellular proliferation and more apoptosis than castrate RC^+ prostate

We found that RC^+ mouse prostate had clearly more Ki-67-positive neoplastic cells (Fig. 3A) than RC^- mouse prostate (Fig. 3B). The differences between RC^+ and RC^- mice were statistically significant in the dorsal prostatic lobes (DP), lateral prostatic lobes (LP), and ventral prostatic lobes (VP) ($P < 0.05$ or $P < 0.01$, Fig. 3C). On the other hand, the number of apoptotic cells as detected by TUNEL staining was fewer in the RC^+ mouse prostatic lobes (Fig. 3D) than in the RC^- mouse prostatic lobes (Fig. 3E), which was statistically significant ($P < 0.01$, Fig. 3F).

Castrate RC$^-$ prostate decreased expression of invasion-related proteins

Previously we reported that the intact RC$^-$ mice expressed significantly less MMP7 in the prostate than the intact RC$^+$ mice, which partially explained the lower rate of invasive cancer in RC$^-$ mice compared to RC$^+$ mice [28]. In the castrate mice, the level of MMP7 expression was also lower in the RC$^-$ prostate than in the RC$^+$ prostate (Fig. 4A and 4B).

To search for other proteins that might contribute to the different incidence rates of invasive cancer in our animal models, we tested several candidates that were reportedly involved in prostate carcinogenesis. YBX1 (also known as YB-1) is a Y-box binding protein [31], which has been demonstrated to confer invasiveness to breast cancer cells [32]. YBX1 level is elevated in human PIN and invasive adenocarcinomas [33], similar to the pattern of MMP7 expression [28]. We found that YBX1 expression was clearly decreased in the castrate RC$^-$ prostate compared to the castrate RC$^+$ prostate (Fig. 4C and 4D). Metastasis associated 1 (MTA1) was originally identified from rat mammary adenocarcinoma cell lines [34] and recently it has been associated with the invasiveness of human prostate cancer cells [35]. We found that MTA1 expression was discernibly decreased in the castrate RC$^-$ prostate compared to the castrate RC$^+$ prostate (Fig. 4E and 4F). Ubiquitin-conjugating enzyme E2C (UBE2C, also called UBCH10) is needed for degradation of mitotic cyclins [36], which has been associated with malignant transformation and aggressiveness of many tumors [37]. UBE2C level is undetectable in human normal prostate, low in hormone-sensitive prostate cancer and high in CRPC [38]. Again, we found that UBE2C level was obviously higher in the castrate RC$^+$ prostate than the castrate RC$^-$ prostate (Fig. 4G and 4H).

Castrate RC$^-$ prostate had less angiogenesis than castrate RC$^+$ prostate

IL-17 has been found to be able to promote migration and cord formation of vascular endothelial cells through induction of a variety of proangiogenic factors [39], thus IL-17 may enhance in vivo lung cancer growth via promoting angiogenesis [40]. By immunohistochemical staining of CD31, we found that there were clearly more blood vessels in the castrate RC$^+$ prostate than in the castrate RC$^-$ prostate (Fig. 5A and 5B), which was statistically significant in the prostatic lobes examined ($P < 0.01$, Fig. 5C). We and other investigators have shown that IL-17 can induce angiogenic CXC chemokines including CXCL1, CXCL5 and CXCL8 expression [28,40]. It has been reported that cyclooxygenase-2 (COX-2) is induced by IL-17 in keratinocytes [41]. In the present study, we found that COX-2 level was dramatically lower in RC$^-$ prostate than RC$^+$ prostate (Fig. 5D and 5E). We also found that hypoxia inducible factor 1-α (HIF1A) level was not discernibly different between RC$^+$ and RC$^-$ prostates (Fig. 5F and 5G). However, the level of vascular endothelial growth factor A (VEGFA) was clearly higher in RC$^+$ prostate than RC$^-$ prostate (Fig. 5H and 5I). It has been demonstrated that the COX-2-VEGF pathway is involved in gastric angiogenesis [42]. Our findings suggest that the COX-2-VEGF pathway plays a role in prostatic angiogenesis while HIF1A's role may be very limited.

Castrate RC$^-$ prostate had less inflammatory cell infiltration than castrate RC$^+$ prostate

Previously we reported that the inflammatory cell population was mainly composed of macrophages (or myeloid cells) and lymphocytes in the intact mouse prostate and the number of inflammatory cells was significantly reduced in RC$^-$ prostate compared to RC$^+$

prostate [28]. In the castrate mouse prostate, the inflammatory cell population was mainly composed of lymphocytes (Fig. 6A). Consistent with our observation in the intact mice, we found that the number of inflammatory cells was much fewer in the castrate RC^- prostate than the castrate RC^+ prostate (Fig. 6A and 6B), which was statistically significant ($P < 0.01$, Fig. 6C).

It has been shown that IL-17 induces infiltration of myeloid-derived suppressor cells (MDSCs) to promote prostate tumor growth [43]. MDSCs are considered as immature myeloid cells that are identified as CD11b/granulocyte-differentiation antigen-1 (Gr-1) double-positive cells. Gr-1 antigen consists of two epitopes recognized by anti-Ly6G (lymphocyte antigen 6 complex, locus G) and anti-Ly6C (lymphocyte antigen 6 complex, locus C). Thus, MDSCs consist of two major subsets: cells with granulocytic phenotype marked by $CD11b^+/Ly6G^+$ and cells with monocytic phenotype marked by $CD11b^+/Ly6C^+$, both subsets having equal suppressive activities against T cell function [44]. Therefore, we examined the infiltration of the two MDSC subsets in mouse prostate. We found that the numbers of both MDSC subsets were significantly reduced in RC^- prostate compared to RC^+ prostate ($P < 0.05$, Fig. 6D to 6I).

It has been reported that the inducible nitric oxide synthase (iNOS)-positive M1 macrophages and arginase I-positive M2 macrophages are present in the mouse prostate tumors, where M1 macrophages have anti-tumor functions while M2 macrophages have pro-tumor functions [45]. We found that there were slightly fewer M1 macrophages than M2 macrophages in both RC^+ and RC^- prostates (Fig. 6J to 6O). Yet, the numbers of M1 and M2 macrophages were significantly reduced in RC^- prostate compared to RC^+ prostate (Fig. 6L and 6O).

DISCUSSION

We previously reported that *Il17rc* knockout inhibited formation and growth of hormone-naïve prostate adenocarcinoma in the *Pten* conditional knockout mouse model [28]. In the present study, we used the same mouse model and castrated the animals at 16 weeks of age. Fourteen weeks after castration, we found that invasive adenocarcinomas were present in both RC^+ and RC^- mouse prostates, albeit at different incidence rates. The GU bloc size, judged by the GU bloc weight, was significantly smaller in the castrate mice than the intact mice (Fig. 1). The remaining invasive adenocarcinomas in the castrate mice presumably are CRPC based on the direct evidence that cellular proliferation was still present 14 weeks after the absence of testicular androgens. Another line of indirect evidence is that UBE2C level was very high in the castrate RC^+ mouse prostate as UBE2C was only expressed at high levels in CRPC [38].

The most significant phenotypic difference between the castrate RC^+ and RC^- mice is the incidence rate of invasive adenocarcinomas. RC^+ mice presented invasive adenocarcinomas in 65% of prostatic glands, in sharp contrast to 23% of prostatic glands in RC^- mice (Fig. 2E). These incidence rates are much lower than the rates in the non-castrate RC^+ and RC^- mice (i.e., 100% and 70%, respectively) [28,29]. One possible reason is that the AR-positive prostatic epithelium undergoes increased apoptosis in response to castration. A 10-times

increase of apoptotic cells in the *Pten*-null prostate cancer was found compared to the intact mouse prostate cancer, and the apoptotic rate was even higher in the prostate cancer than the normal epithelium 3 days post-castration [29]. Apoptosis may possibly lead to regression of some invasive adenocarcinomas and PIN lesions, resulting in a heterogeneous appearance of normal epithelium, PIN, and invasive adenocarcinomas.

There are several possible reasons to explain the different incidence rates of invasive adenocarcinomas between the castrate RC^+ and RC^- mice. First, the cellular proliferation rate is higher in RC^+ prostate than RC^- prostate while the apoptotic rate is lower in RC^+ prostate than RC^- prostate. These differences confer an advantage to the tumor growth in RC^+ mice over RC^- mice. Second, several proteins, namely, MMP7, YBX1, MTA1, and UBE2C, are expressed at higher levels in RC^+ prostate than RC^- prostate. These proteins have been associated with the invasiveness and aggressiveness of human prostate cancer cells [28,32,33,35,38]. While we have demonstrated that MMP7 is a direct downstream target of IL-17 signaling pathway [28], it remains to be determined if YBX1, MTA1, and UBE2C are also IL-17 downstream targets. Third, angiogenesis is reduced in RC^- prostate compared to RC^+ prostate. Angiogenesis is an integral hallmark of cancer and it has recently been associated with early neoplastic progression besides its well-known role in macroscopic tumors [46]. One mechanism by which IL-17 promotes lung cancer growth is through induction of angiogenesis [40]. The reduced levels of COX-2 and VEGFA in RC^- prostate may be responsible for the decreased angiogenesis, as the COX-2-VEGF pathway has been associated with gastric angiogenesis [42]. COX-2 is an IL-17 downstream target in keratinocytes [41]. And last, inflammatory cell infiltration is reduced in RC^- prostate compared to RC^+ prostate. The number of inflammatory cells appears to be more in the prostate of the castrate mice than the intact mice. It has been reported that androgen ablation increased infiltration of CD4+ T cells and macrophages in human prostate tumors [47]. The inflammatory cell population shifts from myeloid cells/lymphocytes in the intact mice to mainly lymphocytes in the castrate mice. This finding is in line with a recent report that castration elicits infiltration of T_H1 cells followed by predominantly T_H17 cells in rat prostate [48]. The subtypes of lymphocytes in our animal models are the subjects of our ongoing studies. Nevertheless, we have shown that the numbers of two major myeloid cell types, MDSCs and macrophages, are significantly reduced in RC^- mice compared to RC^+ mice. We have recently demonstrated that IL-17 is a chemoattractant for monocytes/macrophages [49]. The reduced infiltration of MDSCs and macrophages may be caused by lack of IL-17RC receptor on these cells and/or indirectly by the decreased chemokine levels in the tumor microenvironment of RC^- mice. Since MDSCs and M2 macrophages are pro-tumor inflammatory cells, a decrease in their numbers may partially contribute to the phenotype of reduced incidence rate of invasive adenocarcinomas in RC^- mice.

In summary, the present study demonstrates that IL-17 promotes development of CRPC in the *Pten* conditional knockout mouse model. IL-17 may affect several hallmark capabilities of cancer, including sustaining proliferation, resisting cell death, activating invasion, inducing angiogenesis, and recruiting pro-tumor inflammatory cells [46]. These findings suggest that blocking IL-17 signaling through pharmacological interventions may have potentials in the prevention and treatment of CRPC.

CONCLUSIONS

IL-17 promotes development of invasive prostate adenocarcinomas in *Pten* conditional knockout mice under castrate conditions, potentially through creating an immunotolerant and pro-angiogenic tumor microenvironment.

Supplementary Material

Refer to Web version on PubMed Central for supplementary material.

Acknowledgments

Grant sponsor: National Institute of General Medical Sciences; Grant number: P20GM103518; and National Cancer Institute; Grant number: R01CA174714; the content of this article is solely the responsibility of the authors and does not necessarily represent the official views of the National Institutes of Health; Grant sponsor: Department of Defense; Grant numbers: PC121647 and PC131448; Grant sponsor: The Developmental Fund of Tulane Cancer Center (TCC) and Louisiana Cancer Research Consortium (LCRC) Fund.

We thank Drs. Prescott L. Deininger, Asim B. Abdel Mageed, Steven M. Hill, David E. Blask, Brian G. Rowan, and Oliver Sartor (Tulane University) for their advices and comments on the manuscript. Tulane Cancer Center Core Facilities were used in this study. We thank Dr. Wenjun Ouyang and Genentech for providing the *Il17rc*$^{-/-}$ mice and NCI MMHCC for providing the PB-Cre4 mice.

ABBREVIATIONS

AR	androgen receptor
Bcl-2	B-cell lymphoma 2
COX-2	cyclooxygenase-2
Cre	Cre recombinase
CRPC	castration-resistant prostate cancer
CXCL	C-X-C motif ligand
GU	genitourinary
Gr-1	granulocyte-differentiation antigen-1
H&E	hematoxylin and eosin
HER-2	human epidermal growth factor receptor 2
HIF	hypoxia inducible factor
IL	interleukin
IL-17RC	IL-17 receptor C
iNOS	inducible nitric oxide synthase
KO	knockout
MDSCs	myeloid-derived suppressor cells
MMP	matrix metalloproteinase
MTA1	metastasis associated 1

PIN	prostatic intraepiethelial neoplasia
Pten	phosphatase and tensin homolog
Ras	rat sarcoma gene
SMA	smooth muscle actin
T_H17	T helpher cells expressing IL-17
TMPRSS2-ERG	transmembrane protease, serine 2 - E-twenty six related gene
TUNEL	terminal deoxynucleotidyl transferase-mediated dUTP nick end labeling
UBE2C	ubiquitin-conjugating enzyme E2C
VEGF	vascular endothelial growth factor
YBX1	Y-box binding protein 1

References

1. Harris WP, Mostaghel EA, Nelson PS, Montgomery B. Androgen deprivation therapy: progress in understanding mechanisms of resistance and optimizing androgen depletion. Nat Clin Pract Urol. 2009; 6(2):76–85. [PubMed: 19198621]
2. Newmark JR, Hardy DO, Tonb DC, Carter BS, Epstein JI, Isaacs WB, Brown TR, Barrack ER. Androgen receptor gene mutations in human prostate cancer. Proc Natl Acad Sci U S A. 1992; 89(14):6319–6323. [PubMed: 1631125]
3. Mohler JL, Gregory CW, Ford OH 3rd, Kim D, Weaver CM, Petrusz P, Wilson EM, French FS. The androgen axis in recurrent prostate cancer. Clin Cancer Res. 2004; 10(2):440–448. [PubMed: 14760063]
4. Hu R, Dunn TA, Wei S, Isharwal S, Veltri RW, Humphreys E, Han M, Partin AW, Vessella RL, Isaacs WB, Bova GS, Luo J. Ligand-independent androgen receptor variants derived from splicing of cryptic exons signify hormone-refractory prostate cancer. Cancer Res. 2009; 69(1):16–22. [PubMed: 19117982]
5. Culig Z, Hobisch A, Cronauer MV, Radmayr C, Trapman J, Hittmair A, Bartsch G, Klocker H. Androgen receptor activation in prostatic tumor cell lines by insulin-like growth factor-I, keratinocyte growth factor, and epidermal growth factor. Cancer Res. 1994; 54(20):5474–5478. [PubMed: 7522959]
6. Craft N, Shostak Y, Carey M, Sawyers CL. A mechanism for hormone-independent prostate cancer through modulation of androgen receptor signaling by the HER-2/neu tyrosine kinase. Nat Med. 1999; 5(3):280–285. [PubMed: 10086382]
7. Debes JD, Schmidt LJ, Huang H, Tindall DJ. p300 mediates androgen-independent transactivation of the androgen receptor by interleukin 6. Cancer Res. 2002; 62(20):5632–5636. [PubMed: 12384515]
8. Jin RJ, Wang Y, Masumori N, Ishii K, Tsukamoto T, Shappell SB, Hayward SW, Kasper S, Matusik RJ. NE-10 neuroendocrine cancer promotes the LNCaP xenograft growth in castrated mice. Cancer Res. 2004; 64(15):5489–5495. [PubMed: 15289359]
9. McDonnell TJ, Troncoso P, Brisbay SM, Logothetis C, Chung LW, Hsieh JT, Tu SM, Campbell ML. Expression of the protooncogene bcl-2 in the prostate and its association with emergence of androgen-independent prostate cancer. Cancer Res. 1992; 52(24):6940–6944. [PubMed: 1458483]
10. July LV, Akbari M, Zellweger T, Jones EC, Goldenberg SL, Gleave ME. Clusterin expression is significantly enhanced in prostate cancer cells following androgen withdrawal therapy. Prostate. 2002; 50(3):179–188. [PubMed: 11813210]

11. Heidenberg HB, Bauer JJ, McLeod DG, Moul JW, Srivastava S. The role of the p53 tumor suppressor gene in prostate cancer: a possible biomarker? Urology. 1996; 48(6):971–979. [PubMed: 8973691]
12. Abate-Shen C, Banach-Petrosky WA, Sun X, Economides KD, Desai N, Gregg JP, Borowsky AD, Cardiff RD, Shen MM. Nkx3. 1; Pten mutant mice develop invasive prostate adenocarcinoma and lymph node metastases. Cancer Res. 2003; 63(14):3886–3890. [PubMed: 12873978]
13. Graff JR, Konicek BW, McNulty AM, Wang Z, Houck K, Allen S, Paul JD, Hbaiu A, Goode RG, Sandusky GE, Vessella RL, Neubauer BL. Increased AKT activity contributes to prostate cancer progression by dramatically accelerating prostate tumor growth and diminishing p27Kip1 expression. J Biol Chem. 2000; 275(32):24500–24505. [PubMed: 10827191]
14. Cai C, Wang H, Xu Y, Chen S, Balk SP. Reactivation of androgen receptor-regulated TMPRSS2:ERG gene expression in castration-resistant prostate cancer. Cancer Res. 2009; 69(15): 6027–6032. [PubMed: 19584279]
15. Tomlins SA, Rhodes DR, Perner S, Dhanasekaran SM, Mehra R, Sun XW, Varambally S, Cao X, Tchinda J, Kuefer R, Lee C, Montie JE, Shah RB, Pienta KJ, Rubin MA, Chinnaiyan AM. Recurrent fusion of TMPRSS2 and ETS transcription factor genes in prostate cancer. Science. 2005; 310(5748):644–648. [PubMed: 16254181]
16. Shi XB, Tepper CG, White RW. MicroRNAs and prostate cancer. J Cell Mol Med. 2008; 12(5A): 1456–1465. [PubMed: 18624768]
17. Sun T, Wang Q, Balk S, Brown M, Lee GS, Kantoff P. The role of microRNA-221 and microRNA-222 in androgen-independent prostate cancer cell lines. Cancer Res. 2009; 69(8):3356–3363. [PubMed: 19351832]
18. Corcoran NM, Costello AJ. Interleukin-6: minor player or starring role in the development of hormone-refractory prostate cancer? BJU Int. 2003; 91(6):545–553. [PubMed: 12656913]
19. Lee LF, Louie MC, Desai SJ, Yang J, Chen HW, Evans CP, Kung HJ. Interleukin-8 confers androgen-independent growth and migration of LNCaP: differential effects of tyrosine kinases Src and FAK. Oncogene. 2004; 23(12):2197–2205. [PubMed: 14767470]
20. Onishi RM, Gaffen SL. Interleukin-17 and its target genes: mechanisms of interleukin-17 function in disease. Immunology. 2010; 129(3):311–321. [PubMed: 20409152]
21. Toy D, Kugler D, Wolfson M, Vanden Bos T, Gurgel J, Derry J, Tocker J, Peschon J. Cutting edge: interleukin 17 signals through a heteromeric receptor complex. J Immunol. 2006; 177(1):36–39. [PubMed: 16785495]
22. Haudenschild D, Moseley T, Rose L, Reddi AH. Soluble and transmembrane isoforms of novel interleukin-17 receptor-like protein by RNA splicing and expression in prostate cancer. J Biol Chem. 2002; 277(6):4309–4316. [PubMed: 11706037]
23. Ely LK, Fischer S, Garcia KC. Structural basis of receptor sharing by interleukin 17 cytokines. Nat Immunol. 2009; 10(12):1245–1251. [PubMed: 19838198]
24. Ye P, Rodriguez FH, Kanaly S, Stocking KL, Schurr J, Schwarzenberger P, Oliver P, Huang W, Zhang P, Zhang J, Shellito JE, Bagby GJ, Nelson S, Charrier K, Peschon JJ, Kolls JK. Requirement of interleukin 17 receptor signaling for lung CXC chemokine and granulocyte colony-stimulating factor expression, neutrophil recruitment, and host defense. J Exp Med. 2001; 194(4):519–527. [PubMed: 11514607]
25. Hu Y, Ota N, Peng I, Refino CJ, Danilenko DM, Caplazi P, Ouyang W. IL-17RC Is Required for IL-17A- and IL-17F-Dependent Signaling and the Pathogenesis of Experimental Autoimmune Encephalomyelitis. J Immunol. 2010; 184(8):4307–4316. [PubMed: 20231694]
26. You Z, Dong Y, Kong X, Zhang Y, Vessella RL, Melamed J. Differential expression of IL-17RC isoforms in androgen-dependent and androgen-independent prostate cancers. Neoplasia. 2007; 9(6):464–470. [PubMed: 17603628]
27. You Z, Shi XB, DuRaine G, Haudenschild D, Tepper CG, Lo SH, Gandour-Edwards R, de Vere White RW, Reddi AH. Interleukin-17 receptor-like gene is a novel antiapoptotic gene highly expressed in androgen-independent prostate cancer. Cancer Res. 2006; 66(1):175–183. [PubMed: 16397230]

28. Zhang Q, Liu S, Ge D, Xue Y, Xiong Z, Abdel-Mageed AB, Myers L, Hill SM, Rowan BG, Sartor O, Melamed J, Chen Z, You Z. Interleukin-17 promotes formation and growth of prostate adenocarcinoma in mouse models. Cancer Res. 2012; 72(10):2589–2599. [PubMed: 22461511]
29. Wang S, Gao J, Lei Q, Rozengurt N, Pritchard C, Jiao J, Thomas GV, Li G, Roy-Burman P, Nelson PS, Liu X, Wu H. Prostate-specific deletion of the murine Pten tumor suppressor gene leads to metastatic prostate cancer. Cancer Cell. 2003; 4(3):209–221. [PubMed: 14522255]
30. Shappell SB, Thomas GV, Roberts RL, Herbert R, Ittmann MM, Rubin MA, Humphrey PA, Sundberg JP, Rozengurt N, Barrios R, Ward JM, Cardiff RD. Prostate pathology of genetically engineered mice: definitions and classification. The consensus report from the Bar Harbor meeting of the Mouse Models of Human Cancer Consortium Prostate Pathology Committee. Cancer Res. 2004; 64(6):2270–2305. [PubMed: 15026373]
31. Didier DK, Schiffenbauer J, Woulfe SL, Zacheis M, Schwartz BD. Characterization of the cDNA encoding a protein binding to the major histocompatibility complex class II Y box. Proc Natl Acad Sci U S A. 1988; 85(19):7322–7326. [PubMed: 3174636]
32. Lovett DH, Cheng S, Cape L, Pollock AS, Mertens PR. YB-1 alters MT1-MMP trafficking and stimulates MCF-7 breast tumor invasion and metastasis. Biochem Biophys Res Commun. 2010; 398(3):482–488. [PubMed: 20599698]
33. Gimenez-Bonafe P, Fedoruk MN, Whitmore TG, Akbari M, Ralph JL, Ettinger S, Gleave ME, Nelson CC. YB-1 is upregulated during prostate cancer tumor progression and increases P-glycoprotein activity. Prostate. 2004; 59(3):337–349. [PubMed: 15042610]
34. Toh Y, Pencil SD, Nicolson GL. A novel candidate metastasis-associated gene, mta1, differentially expressed in highly metastatic mammary adenocarcinoma cell lines. cDNA cloning, expression, and protein analyses. J Biol Chem. 1994; 269(37):22958–22963. [PubMed: 8083195]
35. Kai L, Wang J, Ivanovic M, Chung YT, Laskin WB, Schulze-Hoepfner F, Mirochnik Y, Satcher RL Jr, Levenson AS. Targeting prostate cancer angiogenesis through metastasis-associated protein 1 (MTA1). Prostate. 2011; 71(3):268–280. [PubMed: 20717904]
36. Townsley FM, Aristarkhov A, Beck S, Hershko A, Ruderman JV. Dominant-negative cyclin-selective ubiquitin carrier protein E2-C/UbcH10 blocks cells in metaphase. Proc Natl Acad Sci U S A. 1997; 94(6):2362–2367. [PubMed: 9122200]
37. Hao Z, Zhang H, Cowell J. Ubiquitin-conjugating enzyme UBE2C: molecular biology, role in tumorigenesis, and potential as a biomarker. Tumour Biol. 2012; 33(3):723–730. [PubMed: 22170434]
38. Wang Q, Li W, Zhang Y, Yuan X, Xu K, Yu J, Chen Z, Beroukhim R, Wang H, Lupien M, Wu T, Regan MM, Meyer CA, Carroll JS, Manrai AK, Janne OA, Balk SP, Mehra R, Han B, Chinnaiyan AM, Rubin MA, True L, Fiorentino M, Fiore C, Loda M, Kantoff PW, Liu XS, Brown M. Androgen receptor regulates a distinct transcription program in androgen-independent prostate cancer. Cell. 2009; 138(2):245–256. [PubMed: 19632176]
39. Numasaki M, Fukushi J-i, Ono M, Narula SK, Zavodny PJ, Kudo T, Robbins PD, Tahara H, Lotze MT. Interleukin-17 promotes angiogenesis and tumor growth. Blood. 2003; 101(7):2620–2627. [PubMed: 12411307]
40. Numasaki M, Watanabe M, Suzuki T, Takahashi H, Nakamura A, McAllister F, Hishinuma T, Goto J, Lotze MT, Kolls JK, Sasaki H. IL-17 enhances the net angiogenic activity and in vivo growth of human non-small cell lung cancer in SCID mice through promoting CXCR-2-dependent angiogenesis. J Immunol. 2005; 175(9):6177–6189. [PubMed: 16237115]
41. Kanda N, Koike S, Watanabe S. IL-17 suppresses TNF-alpha-induced CCL27 production through induction of COX-2 in human keratinocytes. J Allergy Clin Immunol. 2005; 116(5):1144–1150. [PubMed: 16275389]
42. Miura S, Tatsuguchi A, Wada K, Takeyama H, Shinji Y, Hiratsuka T, Futagami S, Miyake K, Gudis K, Mizokami Y, Matsuoka T, Sakamoto C. Cyclooxygenase-2-regulated vascular endothelial growth factor release in gastric fibroblasts. Am J Physiol Gastrointest Liver Physiol. 2004; 287(2):G444–451. [PubMed: 15246970]
43. He D, Li H, Yusuf N, Elmets CA, Li J, Mountz JD, Xu H. IL-17 promotes tumor development through the induction of tumor promoting microenvironments at tumor sites and myeloid-derived suppressor cells. J Immunol. 2010; 184(5):2281–2288. [PubMed: 20118280]

44. Youn JI, Nagaraj S, Collazo M, Gabrilovich DI. Subsets of myeloid-derived suppressor cells in tumor-bearing mice. J Immunol. 2008; 181(8):5791–5802. [PubMed: 18832739]
45. Redente EF, Dwyer-Nield LD, Merrick DT, Raina K, Agarwal R, Pao W, Rice PL, Shroyer KR, Malkinson AM. Tumor progression stage and anatomical site regulate tumor-associated macrophage and bone marrow-derived monocyte polarization. Am J Pathol. 2010; 176(6):2972–2985. [PubMed: 20431028]
46. Hanahan D, Weinberg RA. Hallmarks of cancer: the next generation. Cell. 2011; 144(5):646–674. [PubMed: 21376230]
47. Mercader M, Bodner BK, Moser MT, Kwon PS, Park ES, Manecke RG, Ellis TM, Wojcik EM, Yang D, Flanigan RC, Waters WB, Kast WM, Kwon ED. T cell infiltration of the prostate induced by androgen withdrawal in patients with prostate cancer. Proc Natl Acad Sci U S A. 2001; 98(25):14565–14570. [PubMed: 11734652]
48. Morse MD, McNeel DG. T cells localized to the androgen-deprived prostate are T(H) 1 and T(H) 17 biased. Prostate. 2012; 72(11):1239–1247. [PubMed: 22213030]
49. Liu L, Ge D, Ma L, Mei J, Liu S, Zhang Q, Ren F, Liao H, Pu Q, Wang T, You Z. Interleukin-17 and prostaglandin E2 are involved in formation of an M2 macrophage-dominant microenvironment in lung cancer. J Thorac Oncol. 2012; 7(7):1091–1100. [PubMed: 22534817]

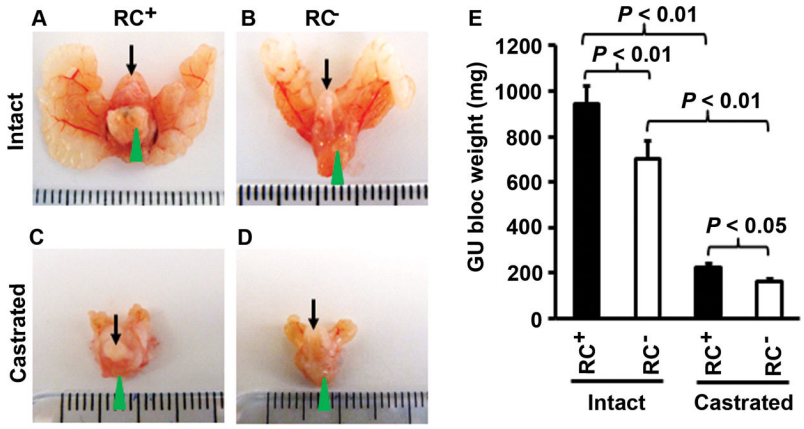

Fig. 1.

Castrate RC^- mice developed smaller prostate glands than castrate RC^+ mice. **A–D:** Representative photographs of the GU blocs; arrows indicate urinary bladders and arrowheads indicate the ventral prostatic lobes for orientation of the view. **E:** The GU bloc weights at 30 weeks of age; n = 20 for intact RC^+ mice, n = 12 for intact RC^- mice, n = 9 for castrate RC^+ mice, and n = 9 for castrate RC^- mice.

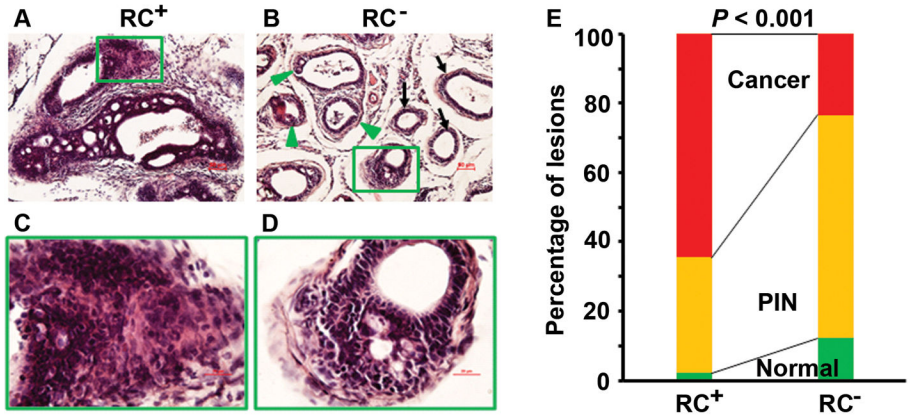

Fig. 2.

Castrate RC^{-} mice developed fewer invasive adenocarcinomas than castrate RC^{+} mice. **AD:** Representatives of H&E-stained dorsal prostatic lobes; arrows indicate normal glands with a single layer of luminal epithelium, arrowheads indicate PIN lesions, and rectangular frames indicate invasive adenocarcinomas; original magnification, x100 for (A–B) and x400 for (C–D). **E:** Percentages of normal, PIN, and invasive cancer in dorsal, lateral, and ventral prostatic lobes.

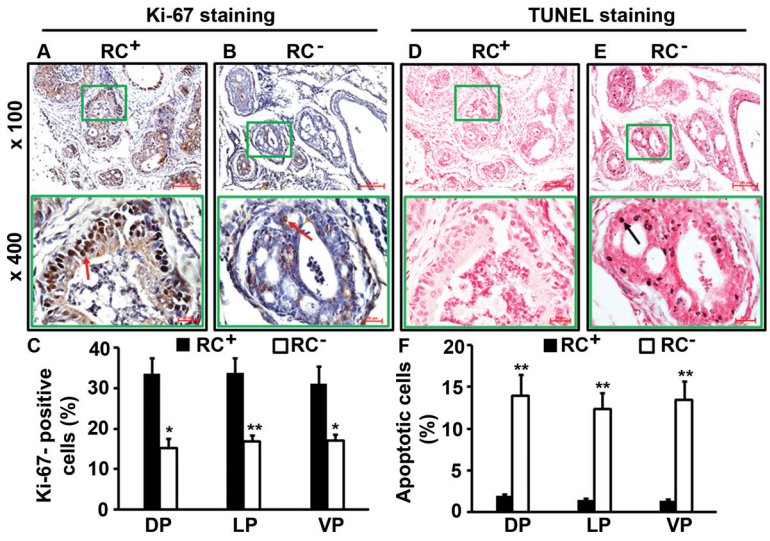

Fig. 3.

Castrate RC^- prostate had less cellular proliferation and more apoptosis than castrate RC^+ prostate. **A–B:** Ki-67 staining; arrows indicate the positive cells. **C:** Percentages of Ki-67-positive cells in dorsal (DP), lateral (LP), and ventral (VP) prostatic lobes; $*P < 0.05$ and $**P < 0.01$. **D–E:** TUNEL staining; arrow indicates the positive cells. **F:** Percentages of apoptotic cells in prostatic lobes; $**P < 0.01$.

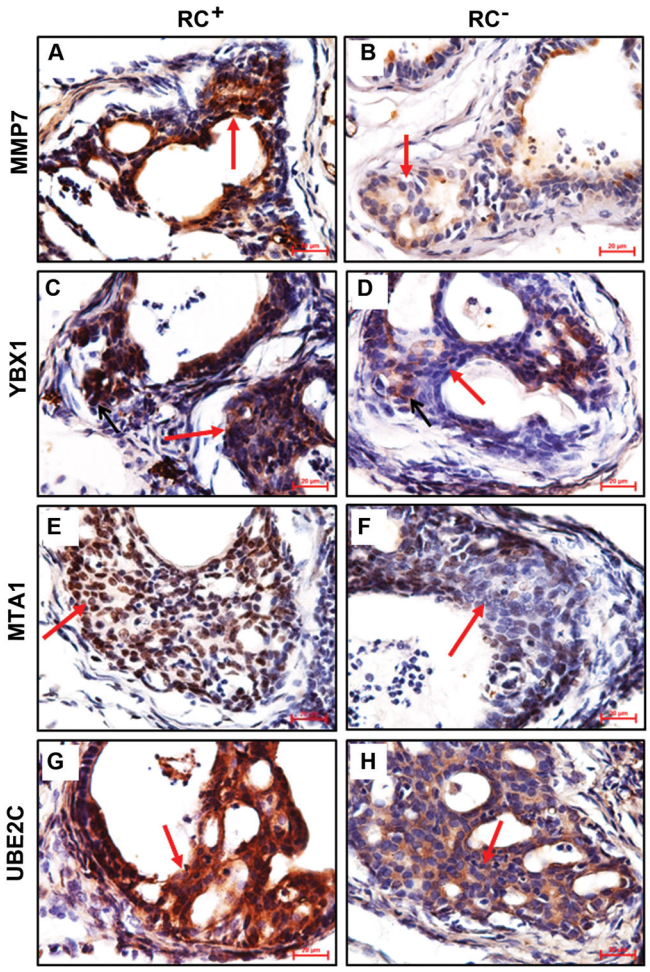

Fig. 4.

Castrate RC⁻ prostate decreased expression of invasion-related proteins. **A–H:** Representatives of immunohistochemical staining; arrows indicate neoplastic cells; original magnification, x400.

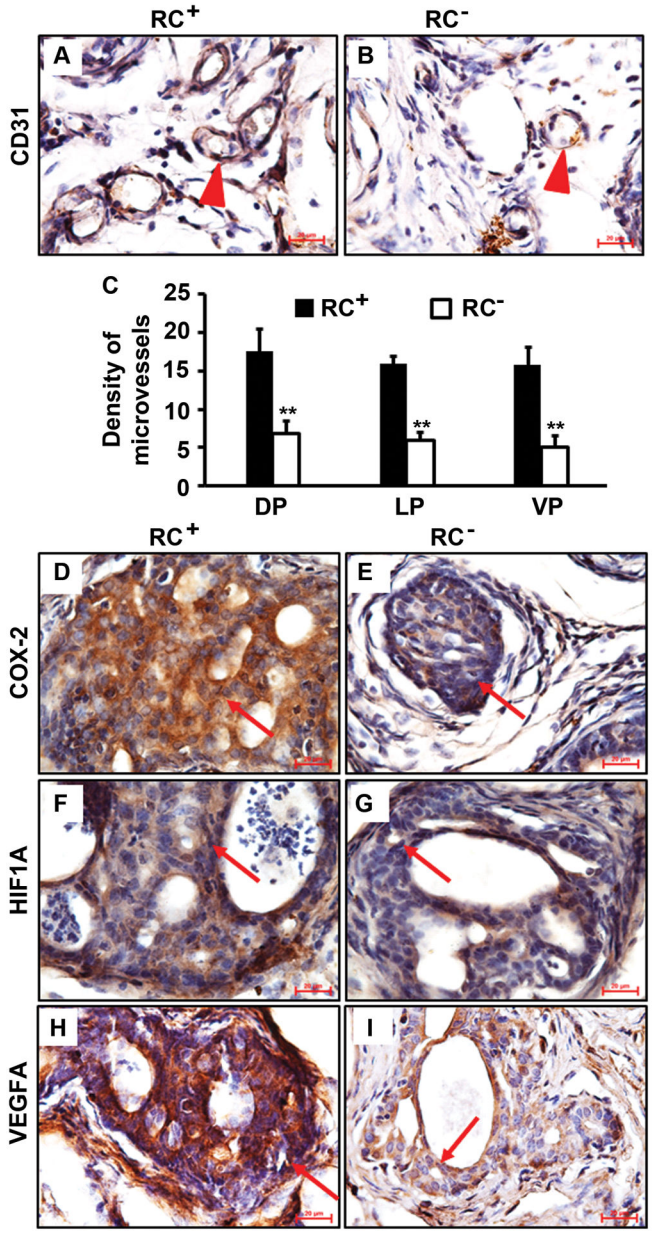

Fig. 5.

Castrate RC^- prostate had less angiogenesis than castrate RC^+ prostate. **A–B:** Representatives of CD31 staining; arrowheads indicate microvessels. **C:** Density of microvessels in prostatic lobes; $^{**}P < 0.01$. **D–I:** Representatives of immunohistochemical staining; arrows indicate neoplastic cells; original magnification, x400.

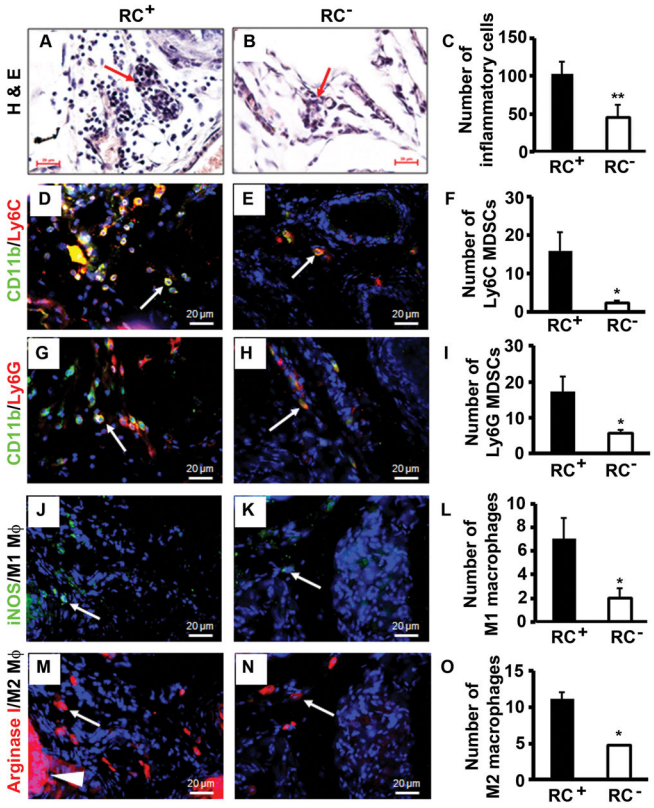

Fig. 6.

Castrate RC^{-} prostate had less inflammatory cell infiltration than castrate RC^{+} prostate. **AB:** H&E staining; arrows indicate lymphocytes. **C:** Number of inflammatory cells counted on H&E-stained sections. **D–E:** Double immunofluorescent staining of CD11b and Ly6C. **F:** Number of Ly6C MDSCs. **G–H:** Double immunofluorescent staining of CD11b and Ly6G. **I:** Number of Ly6G MDSCs. **J–K:** Immunofluorescent staining of iNOS-positive M1 macrophages. **L:** Number of M1 macrophages. **M–N:** Immunofluorescent staining of arginase I-positive M2 macrophages; arrowhead indicates positively stained prostatic epithelium. **O:** Number of M2 macrophages. Original magnification, x400; arrows indicate positive cells; $*P < 0.05$ and $**P < 0.01$.